

## REPORT DOCUMENTATION PAGE

AFRL-SR-BL-TR-01-

Public reporting burden for this collection of information is estimated to average 1 hour per response, including gathering and maintaining the data needed, and completing and reviewing the collection of information. Send collection of information, including suggestions for reducing this burden, to Washington Headquarters Service, Davis Highway, Suite 1204, Arlington, VA 22202-4302, and to the Office of Management and Budget, Paper

ces,  
this  
rson

0057

1. AGENCY USE ONLY (Leave blank)		2. REPORT DATE		3. REPORT TYPE AND DATES COVERED Final 01 Jun 97 to 31 Oct 00	
4. TITLE AND SUBTITLE Atmospheric Pressure Plasma and Electron Cyclotron Resonance Plasma and Their Applications				5. FUNDING NUMBERS 2301/EX 61102F	
6. AUTHOR(S) Dr. Kuo					
7. PERFORMING ORGANIZATION NAME(S) AND ADDRESS(ES) Polytechnic University Dept of Electrical Engineering 901 Route 110 Farmingdale, NY 11735				8. PERFORMING ORGANIZATION REPORT NUMBER	
9. SPONSORING/MONITORING AGENCY NAME(S) AND ADDRESS(ES) Air Force Office of Scientific Research 801 N. Randolph Street Arlington, VA 22203-1977				10. SPONSORING/MONITORING AGENCY REPORT NUMBER  F49620-97-1-0294	
11. SUPPLEMENTARY NOTES					
12a. DISTRIBUTION AVAILABILITY STATEMENT Unlimited Distribution		AIR FORCE OFFICE OF SCIENTIFIC RESEARCH (AFOSR) NOTICE OF TRANSMITTAL DTIC. THIS TECHNICAL REPORT HAS BEEN REVIEWED AND IS APPROVED FOR PUBLIC RELEASE LAW AFR 190-12. DISTRIBUTION IS UNLIMITED.			
13. ABSTRACT (Maximum 200 words)  The installation of an array of plasma torches is made easy by introducing a cylindrically shaped plasma torch module, which has been designed and constructed by remodeling components from two commercially available spark plugs and adding a tungsten wire as the central electrode. Use of modules as building blocks of a large volume plasma source also makes easy to the maintenance of the plasma source. This plasma torch module has been improved by adding a dc magnetic field between the electrodes, changing the geometry of the gas plenum chamber for allowing higher gas flow rate, and the shape and position of the central electrode.					
14. SUBJECT TERMS				15. NUMBER OF PAGES	
				16. PRICE CODE	
17. SECURITY CLASSIFICATION OF REPORT  Unclassified		18. SECURITY CLASSIFICATION OF THIS PAGE  Unclassified		19. SECURITY CLASSIFICATION OF ABSTRACT  Unclassified	
				20. LIMITATION OF ABSTRACT  UL	

DTIC QUALITY INSPECTED 1

Standard Form 298 (Rev. 2-89) (EG)  
Prescribed by ANSI Std. Z39.18  
Replaces GSA FPMR (41 CFR) 101-11.6

# **Polytechnic**

## **UNIVERSITY**

Technical Final Report

on

“Atmospheric Pressure Plasma and Electron Cyclotron Resonance  
Plasma and Their Applications”

Submitted by

Professor Spencer Kuo, Principal Investigator

Daniel Bivolaru, Research Fellow

Department of Electrical Engineering  
Polytechnic University  
901 Route 110  
Farmingdale, NY 11735

Prepared For  
Air Force Office of Scientific Research  
Grant No. AFOSR F49620-97-1-0294  
June 1, 1997 to Oct. 31, 2000

20010221 027

# Atmospheric Pressure Plasma and Electron Cyclotron Resonance Plasma and Their Applications

## Executive Summary

The installation of an array of plasma torches is made easy by introducing a cylindrically shaped plasma torch module, which has been designed and constructed by remodeling components from two commercially available spark plugs and adding a tungsten wire as the central electrode. Use of modules as building blocks of a large volume plasma source also makes easy to the maintenance of the plasma source.

This plasma torch module has been improved by adding a dc magnetic field between the electrodes, changing the geometry of the gas plenum chamber for allowing higher gas flow rate, and the shape and position of the central electrode. The improved performance of the new torch module has been evaluated in terms of the plasma parameters and its stability in the operation of an array. It has also been demonstrated that the magnetized torch module can operate with a supersonic flow. A close collaboration with Dr. Skip Williams at AFRL, Hanscom, to evolve our plasma torch module into an Igniter for the high-speed combustor is on going.

The research effort included (1) developing a plasma torch module which is now pending on a patent application, (2) setting up a torch array to demonstrate the feasibility of an array operation, (3) developing new diagnostic techniques for measuring the plasma density and temperature, (4) characterizing the physical parameters of the plasma, and (5) exploring some of the potential applications of the torch plasma, such as applying it for microwave absorption and for supersonic aircraft drag reduction. It was conducted by Professor Spencer Kuo as the PI, and two graduate students, Ed Koretzky, who received Ph.D. degree in 1999, and Daniel Bivolaru, who is expected to complete the Ph.D. degree requirements in 2001.

## I. Introduction

Starting in July 1997, Air Force Office of Scientific Research has awarded a three year research grant (AFOSR-F49620-97-1-0294) entitled "Atmospheric Pressure Plasma and Electron Cyclotron Resonance Plasma and Their Applications" to Polytechnic University with Professor Spencer Kuo as the Principal Investigator. This grant was extended for six months with no additional cost to complete the original proposed work. From the support of this grant, a basic research on exploring the physical processes and engineering merits of "Atmospheric Pressure Plasmas" has been pursued. This research effort is closely related to the MURI program on "Plasma Ramparts". The development of atmospheric-pressure plasma sources, which do not need vacuum systems in their setups and have open structures exposing plasmas directly to the atmosphere, has recently received considerable attention. Their potential applications include the uses of such plasmas for: microwave reflector/absorber<sup>1,2</sup>, sterilization<sup>3-5</sup>, material processings<sup>6,7</sup>, and supersonic aircraft drag reduction<sup>8-10</sup>, etc. The plasmas are characterized by their density, temperature, and volume, which are the required parameters in many of the applications. In addition, power budget is also a practical concern in the applications. Therefore, the basic physical and engineering issues such as (1) how can a low temperature ( $< 2000$  K) high density ( $> 10^{13}$  electrons/cm<sup>3</sup>) plasma with a sizable volume be generated effectively, (2) what are the proper diagnostics for plasma parameters, (3) how can the power budget requirement be minimized, (4) what are the key parameters and processes that can drastically improve the performance of the developed plasma source, and (5) applications, have been explored in this research effort.

An array of plasma torches as a source of producing a large volume atmospheric pressure plasma has been developed. The produced plasma has a density of the order of  $10^{13}$  electrons/cm<sup>3</sup> and a temperature  $T$  less than 2000K. Many of research efforts have yielded useful results, which have been reported in conferences and workshops and published in the journals and proceedings.

The research efforts included (1) developing a plasma torch module<sup>11</sup> which is now pending on a patent application, (2) setting up a torch array to demonstrate the feasibility of an array operation, (3) developing new diagnostic techniques for measuring the plasma

density and temperature<sup>12</sup>, (4) characterizing the physical parameters of the plasma, and (5) determining the operation conditions of the torch array for achieving efficient generation and stable maintenance of the plasma. Moreover, some of the potential applications of the torch plasma, such as applying it for microwave absorption and for supersonic aircraft drag reduction, were explored. In the following section, the works completed and noticable efforts during the past three and a half years under the AFOSR funding support are summarized.

## II. Summary of Works Accomplished from AFOSR Sponsored Research Program:

### A. Publications

1. E. Koretzky and S. P. Kuo, Characterization of an atmospheric pressure plasma generated by a plasma torch array, *Phys. Plasmas*, 5(10), 3774-3780, 1998.
2. K. L. Kelly, J. E. Scharer, G. Ding, M. Bettenhausen, and S. P. Kuo, Microwave reflections from a vacuum ultraviolet laser produced plasma sheet, *J. Appl. Phys.*, 85(1), 63-68, 1999.
3. S. P. Kuo, E. Koretzky, and L. Orlick, Design and electrical characteristics of a modular plasma torch, *IEEE Trans. Plasma Sci.*, 27(3), 752-758, 1999.
4. S. P. Kuo, E. Koretzky, and R. J. Vidmar, Temperature Measurement of an Atmospheric-Pressure Plasma Torch, *Rev. Sci. Instruments*, 70(7), 3032-3034, 1999.
5. S. P. Kuo, I. M. Kalkhoran, D. Bivolaru, and L. Orlick, Observation of Shock Wave Elimination by a Plasma in a Mach-2.5 Flow, *Physics of Plasmas*, 7(5), 1345-1348, 2000.
6. E. Koretzky and S. P. Kuo, Simulation Study of a Capacitively Coupled Plasma Torch Array, *IEEE Trans. Plasma Sci.*, accepted for publication.
7. S. P. Kuo and Daniel Bivolaru, The effect of plasma aerodynamics on shock waves, submitted to the *Physics of Plasmas*.
8. S. P. Kuo, Daniel Bivolaru, Lester Orlick, Igor Alexeff, and D. K. Kalluri, A transmission line filled with fast switched periodic plasma as a wideband frequency transformer, submitted to the *IEEE Trans. Plasma Sci.*.
9. S. P. Kuo, L. Orlick, and E. Koretzky, Design of a modular plasma torch and Its Interaction with Microwaves, AIAA 30th Plasmadynamics and Lasers Conf., AIAA99-3724, 1999.
10. S. P. Kuo, E. Koretzky, and R. J. Vidmar, Analysis of a Melting Wire Temperature Probe Applied to a Plasma Torch, AIAA 30th Plasmadynamics and Lasers Conf., AIAA99-3435, 1999.

11. S. P. Kuo and E. Koretzky, Model and Simulation of a Capacitively Coupled Plasma Torch Array, AIAA 30th Plasmadynamics and Lasers Conf., AIAA99-3435, 1999.
12. S. P. Kuo, I. M. Kalkhoran, D. Bivolaru, and L. Orlick, Experimental observation of plasma aerodynamic effect on shock wave, *ME100 Symposium on Technology for the next century*, Nov. 4-5, 1999.

***B. Patent Application:***

S. P. Kuo, E. Koretzky, and L. Orlick, "A Modular Plasma Torch", application # 60/111,687.

***C. Training of Students:***

(a) Ed Koretzky received Ph.D degree in June, 1999. Research work on plasma Ramparts constitutes a major part of his dissertation. He is now working at TRW Electronics System & Technology Division, Redondo Beach, CA.

(b) Daniel Bivolaru is a graduate student working on the research project. He has passed the preliminary Ph.D qualify examination, progressed satisfactorily in research, and completed the course requirement.

### III. Brief Description of Works Accomplished

A Modular plasma torch has been designed. It has been used as a unit to set up an array of plasma torches as a source of a large volume and dense atmospheric pressure plasma. A thorough study on the characterization of such an atmospheric pressure plasma has been conducted. Several applications of torch plasmas have also been explored. The specific tasks, which we have performed during the funding period, are discussed in the following.

#### 1. Generation and Characterization of a Large Volume Atmospheric Pressure Plasma by a Plasma Torch Array:

Based on a capacitively coupled electrical discharge scheme, it is demonstrated that an array of plasma torches can be lit up simultaneously to form a dense plasma layer in the open air by a single ac power source. Shown in Fig. 1 is a demonstration of an array of three plasma torches lit up simultaneously by a single power supply. The number of torches is only limited by the power handling capability of this source. Using an array arrangement the plasma, in principle, can be produced to fill a desired volume or to cover a desired surface. The measured v-i characteristic of the discharge indicates that the torch is operating in the diffuse arc mode. Experiments have been performed to explore the effect of the plasma torches on the propagation of microwaves in an X-band rectangular waveguide by passing the plasma of the torches through holes on the top and bottom walls of the waveguide. The signals received at the other end of the waveguide are monitored with a spectrum analyzer (HP8569B). The results show that plasma torches can effectively attenuate microwaves. The wave-plasma interaction process is also analyzed analytically and numerically. The plasma parameters deduced from the theoretical model, by matching the numerical results with those of experiments, are shown to agree well with the experimental measurements, that obtain the maximum plasma density in the order of  $3 \times 10^{13} \text{ cm}^{-3}$  and temperature less than 2000 K.

#### 2. Design and Electrical Characteristics of a Modular Plasma Torch and Its Interactions with Microwaves :

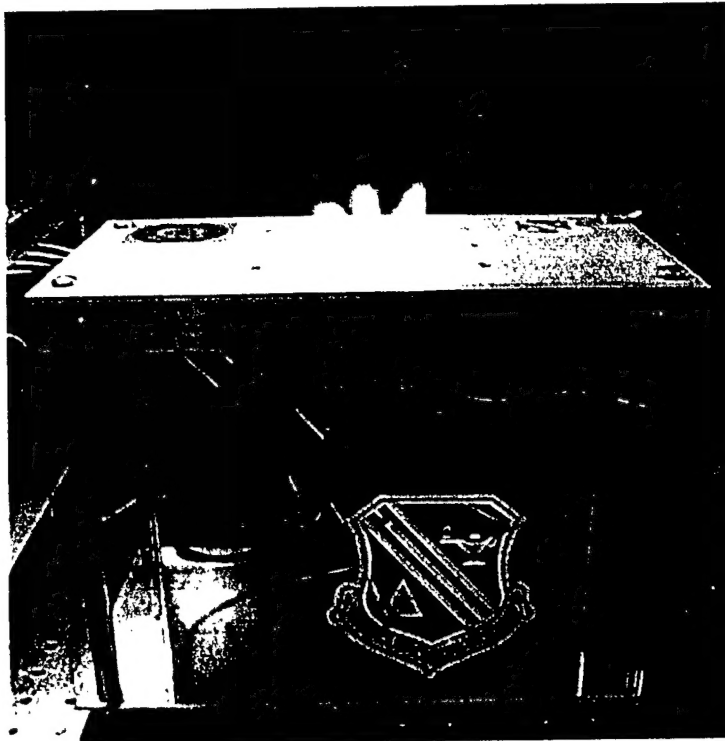


Fig. 1 A photo of three plasma torches produced by a portable array.

The design and construction of a plasma torch module by modifying and reassembling the structural components of two different models of spark plugs are described. Each module can produce a torch plasma of 1 cm radius and 6 cm height and having a peak density exceeding  $10^{13} \text{ cm}^{-3}$ . A set of modules, each connected in series with a ballasting capacitor in the circuit, can be operated as an array sharing a common power source to produce a dense and large volume plasma. The electrical characteristics of the module are studied. It is shown that the discharge can be maintained, with the aid of a series ballasting capacitors, in a stable diffuse arc. The installation of an array of plasma torches is made easy by using modules, which are in cylindrical shape and can easily be mounted on a ground plate. Microwave-plasma interaction is studied in an X-band waveguide by passing the plasma from the torch through pairs of aligned holes on the top and bottom walls of the waveguide. The results show that each torch plasma acting as a lossy dielectric post, can introduce more than 10 dB attenuation to the passing through microwaves.

### 3. Development and Characterization of a Magnetized Plasma Torch Module:

A surface gap spark plug, which has a concentric electrode pair, is used as a frame to construct a plasma torch module. The axial dc magnetic field of the torch module is provided by a ring-shaped permanent magnet. It has an outer diameter of 5.56 cm, an inner diameter of 2.06 cm, and a thickness of 1.07 cm, which is positioned concentrically around the outer electrode (cathode) of the module and held inside an annular chamber as shown in Fig. 2. This annular chamber is also used to replace the gas plenum chamber in the original module. It is found that with the added magnetic field the discharge can now be sustained in a much higher gas flow speed. Therefore, the number of holes drilled through the base of the plug is doubled (from 4 to 8) to increase gas flow rate through the gap between the electrodes.

This magnetic field introduced by the magnet is in the (axial) direction perpendicular to the (radial directed) discharge electric field. It rotates the discharge around the electrodes (in the azimuth direction). Consequently, it enhances the strength (e.g., density and allowable gas flow speed) and stability (e.g., of the shape) of a plasma torch produced by the plasma torch module, and the lifetime of the electrodes by avoiding

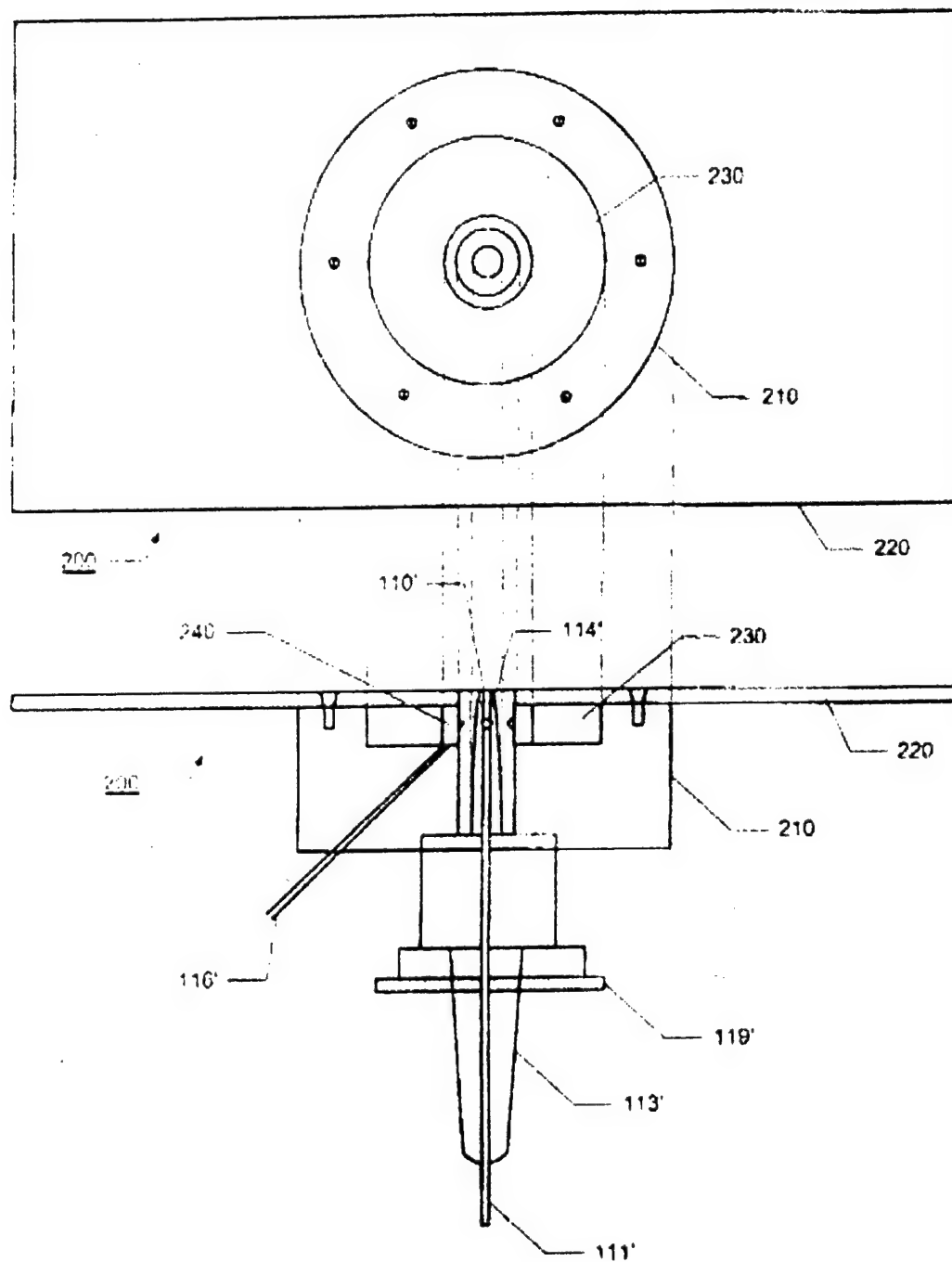


**Fig. 2** A print of the design of magnetized plasma torch module.

discharge at a fixed hot spot. A systematic testing has been made to determine the characteristics of this single torch plasma produced by a magnetized plasma torch module. It has also been demonstrated that the magnetized torch module can operate with a supersonic flow.

#### 4. Analysis of a Melting Wire Temperature Probe Applied to a Plasma Torch:

A simple method to make a temperature measurement in an atmospheric pressure plasma torch with a density of  $10^{13}$  electrons/cm<sup>3</sup> is developed. The method is based on thermal equilibrium and a detail analysis of heat loss from a copper wire placed in a torch. The wire diameter, which regulates heat loss, is systematically reduced to increase the temperature of the wire segment in the torch. At a critical wire diameter, the wire is about to melt suggesting that its temperature in the torch is reaching to the wire melting temperature. This temperature and an analysis of heat input from the torch and heat loss from the wire combine to provide a useful although approximate temperature measurement in the 1300-2200 K range. Using this technique, the temperature of a plasma torch was determined to be approximately 1760 K.

## 5. Other Diagnostics:

### *(a) Laser Measurement of Plasma Dimensions*

A He-Ne laser is used to measure the dimensions of the plasma torch. It is done by moving the torch across the laser beam, which is monitored by a photomultiplier. The density of the background gas is expected to be reduced by the heating of the torch in order to keep pressure balance with the surrounding air. Thus the torch can introduce Rayleigh scattering to the passing through laser beam. Moreover, the metallic vapor from the electrodes can further enhance the Rayleigh scattering. Therefore, a reduction in the monitored laser intensity indicates the presence of the torch in the path of the laser beam. Using a pinhole and a monochromator, the detection system is made extremely sensitive to the presence of the torch, which can cause up to 70% intensity reduction. The results of measurements show that the cylindrically shaped torch has a diameter of 2 cm and a height of 6 cm. The diameter of the torch is mainly determined by the size of the torch module. The height of the torch can, however, increase slightly by increasing the gas flow rate.

### *(b) Power Measurement*

The voltage and current of the discharge of a torch have been measured directly in time. Their product provides the most direct measurement of the power consumption of the torch as well as the other plasma sources. The average power of a single torch is found to be about 300 W. However, a large negative instantaneous power has been measured during a small time interval in each cycle. This negative power reduces the average power considerably.

## 6. Simulation Study of a Capacitively Coupled Plasma Torch Array:

Using capacitively coupled electrical discharges, an array of three plasma torches powered by a single 60 Hz source are lit up simultaneously to produce a dense plasma in the open air. The discharge voltage and current of each torch is measured for three cases of one to three torches being lit up in the array. The results determine the  $v-i$  characteristic of the discharge which indicates that the torch is operating in a diffuse arc mode. The torch array is modeled by an equivalent circuit for simulating its operation. The simulation results of the discharge voltage and current of a torch are shown to agree well with those from the experimental measurements for the three cases. The lump circuit

model is then used to carry out numerical simulations of the discharge for a broad parameter space of plasma species. By fitting the simulation results, a function giving the parametric dependence of the consumed average power density  $\langle P \rangle$  on the normalized average electron density  $\langle n_e \rangle$  maintained in the plasma is determined to be  $\langle P \rangle = 48 \langle n_e \rangle^{1.9} \underline{\alpha}^{0.4}$  (W/cm<sup>3</sup>), where  $\langle n_e \rangle$  is normalized to 10<sup>13</sup> cm<sup>-3</sup> and  $\underline{\alpha}$ , the electron-ion recombination coefficient normalized to 10<sup>-7</sup> cm<sup>3</sup>sec<sup>-1</sup>, is used as a variable parameter

#### 7. Observation of Shock Wave Elimination by a Plasma in a Mach-2.5 Flow:

An experimental study on the influence of a plasma on the structure of an attached conical shock front appearing at the front end of a missile-shaped model has been carried out in a Mach-2.5 flow. The tip and the body of the model are designed as the cathode and anode for gaseous discharge, which produces a spray-like plasma moving around the tip. It is observed that the plasma has caused the shock front to separate from the model. The shock wave moves upstream in the form of a detached bow shock a sensible distance away from the model tip. The detached shock front appears to be highly dispersed in its new location as seen in the shadow video graphs of the flow. As the discharge current increases, experimental evidence shown in the video further reveals a distinct state of the flow without the presence of any shock wave.

#### 8. The Effect of Plasma Aerodynamics on Shock Waves:

in the simulation.

An experimental study of the plasma effect on the structure of an attached conical shock front appearing at the front end of a missile-shaped model has been carried out in a Mach-2.5 stream. The tip and the body of the model are designed as the cathode and anode, which are separated by a conical-shaped ceramic insulator providing a 5-mm gap for gaseous discharge. The electric field intensity near the cathode is enhanced by the sharpness of the tip. The experimental results show that the discharge can produce plasma distributed symmetrically around the tip in the region in front of the shock wave. It is observed that such plasma can caused the shock front to separate from the model. The shock wave moves upstream in the form of a detached bow shock becoming more and

more diffusive and having an increasing shock angle as seen in the shadow video graphs of the flow. A physical mechanism of the observed plasma effect on shock wave is presented.

#### 9. A Transmission Line Filled with Fast Switched Periodic Plasma as a Wideband

##### Frequency Transformer:

A theory is first presented to show the enhancing effects of a periodic structure and a magnetic field on wave frequency-shifting process by a rapidly produced plasma. A device having a cylindrical coaxial line configuration and featuring with a periodic cusp magnetic field, is then constructed to study the theoretically predicted time-domain wave phenomena. The magnetic field is introduced by ring-shaped permanent magnets installed outside the outer cylinder of the coax in an arrangement with alternating polarities. A rapid discharge by a rectangular voltage pulse between the center conductor and the outer cylinder of the coax generates a periodically distributed plasma inside the coax. As an x-band test wave is introduced to propagate through the line, it is shown that the wave frequency is shifted both upward and downward by the suddenly created periodically distributed plasma. The effectiveness of the magnetic field (periodic as well as uniform distribution) on broadening the power spectra of frequency-shifted waves is demonstrated by comparing the spectra for the magnetized cases with that for the unmagnetized case.

#### IV. References

1. R. J. Vidmar, "On the Use of Atmospheric Pressure Plasmas as Electromagnetic Reflectors and Absorbers," *IEEE Trans. Plasma Sci.*, vol. 18, pp. 733-741, 1990.
2. E. Koretzky and S. P. Kuo, "Characterization of an Atmospheric Pressure Plasma Generated by a Plasma Torch Array," *Phys. Plasmas*, vol. 5, pp. 3774-3780, 1998.
3. M. Laroussi, "Sterilization of Contaminated Matter with an Atmospheric Pressure Plasma," *IEEE Trans. Plasma Sci.*, vol. 24, pp. 1188-1191, 1996.
4. K. Kelly Wintenberg, T. C. Montie, C. Brickman, J. R. Roth, A. Carr, K. Sorge, L. Wadsworth, and P. Tsai, "Room Temperature Sterilization of Surfaces and Fabrics with a One Atmosphere Uniform Glow Discharge Plasma," *J. Industrial Microbiol. Biotechnol.*, vol. 20, pp. 69-74, 1998.
5. Special Issue of the *IEEE Transactions on Plasma Science*, vol. 28, February 2000.
6. M. I. Boulos, "Thermal Plasma Processing," *Pure Appl. Chem.*, vol. 57, pp. 1321-1357, 1985.
7. J. R. Roth, "Industrial Plasma Engineering: Vol. I—Principles," *Institute of Phys. Press, Bristol, UK*, pp. 453-461, 1995.
8. V. P. Gordeev, A. V. Krasilnikov, V. I. Lagutin, and V. N. Otmennikov, "Plasma Technology for Reduction of Flying Vehicle Drag," *Fluid Dynamics*, 31, 313, 1996.
9. B. N. Ganguly, P. Bletzinger, and A. Garscadden, "Shock Wave Dumping and Dispersion in Nonequilibrium Low Pressure Argon Plasma," *Phys. Lett. A*, 230, 218, 1997.
10. S. P. Kuo, I. M. Kalkhoran, D. Bivolaru, and L. Orlick, "Observation of Shock Wave Elimination by a Plasma in a Mach-2.5 Flow," *Phys. Plasmas*, vol. 7, 2000.
11. S. P. Kuo, E. Koretzky, and L. Orlick, "Design and Electrical Characteristics of a Modular Plasma Torch," *IEEE Trans. Plasma Sci.*, vol. 27, pp. 752-758, 1999.
12. S. P. Kuo, E. Koretzky, and R. J. Vidmar, "Temperature Measurement of an Atmospheric-Pressure Plasma Torch," *Rev. Sci. Instruments*, vol. 70, pp. 3032-3034, 1999.

## V. Appendices:

1. Simulation Study of a Capacitively Coupled Plasma Torch Array, IEEE Trans. Plasma Sci., accepted for publication.
2. The effect of plasma aerodynamics on shock waves, submitted to the Physics of Plasmas.

# Simulation Study of a Capacitively Coupled Plasma Torch Array

E. Koretzky

Antenna Systems Department, TRW Space & Electronics Group, Redondo Beach, CA

S. P. Kuo

Department of Electrical Engineering, Polytechnic University, Farmingdale, NY

## Abstract

Using capacitively coupled electrical discharges, an array of three plasma torches powered by a single 60 Hz source are lit up simultaneously to produce a dense plasma in the open air. The discharge voltage and current of each torch is measured for three cases of one to three torches being lit up in the array. The results determine the  $v$ - $i$  characteristic of the discharge which indicates that the torch is operating in a diffuse arc mode. The torch array is modeled by an equivalent circuit for simulating its operation. The simulation results of the discharge voltage and current of a torch are shown to agree well with those from the experimental measurements for the three cases. The lump circuit model is then used to carry out numerical simulations of the discharge for a broad parameter space of plasma species. By fitting the simulation results, a function giving the parametric dependence of the consumed average power density  $\langle P \rangle$  on the normalized average electron density  $\langle n_e \rangle$  maintained in the plasma is determined to be  $\langle P \rangle = 48 \langle n_e \rangle^{1.9} \alpha^{0.4}$  (W/cm<sup>3</sup>), where  $\langle n_e \rangle$  is normalized to 10<sup>13</sup> cm<sup>-3</sup> and  $\alpha$ , the electron-ion recombination coefficient normalized to 10<sup>-7</sup> cm<sup>3</sup>sec<sup>-1</sup>, is the used as a variable parameter in the simulation.

## I. INTRODUCTION

Recently there is a considerable interest in atmospheric-pressure plasma sources, which do not need vacuum systems in their setups. Such sources have open structures exposing plasmas directly to the atmosphere. They have the potential applications for microwave reflector/absorbers [1,2], plasma-assisted material processing [3,4], plasma induced sterilization and chemical neutralization [5], and wave drag reduction of the supersonic and hypersonic flights [6]. Most of the applications require that the plasma be dense and large volume. The power budget is also a major concern.

A dense atmospheric-pressure plasma can be produced through a low frequency discharge operating in the high current diffused arc mode, such as a plasma torch which introduces a gas flow to carry the plasma out of the discharge region. However, the volume of a single torch is, generally, not large enough for most of the applications. A simple way to enlarge the plasma volume is by introducing an array of torches as a plasma source. To keep the size of the source compact, the torches of the array have to be coupled to each other so that the number of power sources needed to operate the array can be reduced considerably. It has been demonstrated that an array of three plasma torches can be lit up simultaneously via capacitive coupling by a single 60 Hz power source [2,7], which employs a power transformer with 1:25 turn ratio to step up the voltage from a wall outlet to 3 kV. Air flow at a speed of about 25 m/s is used in the torch operation to keep the discharge in the diffused form and to optimize the height of the torch. The density and temperature of the torch plasma were measured. The density of the plasma varies in time (at 120 Hz) and has a peak value around  $10^{13}$  electrons/cm<sup>3</sup> [2]. The torch plasma is in thermal equilibrium with the background gas and has a peak temperature of about 1800 K [8] in the region near the electrodes. It is noted that the torch plasma is not steady state in time and ionization is maintained by an electric field distributed in the background in addition to the thermal ionization process. The images of a fast CCD camera show that the current path of the discharge has a spatial distribution, which varies in time and covers the entire region of the torch plasma. It explains why such a high density air plasma can be maintained at a considerably low temperature.

In the preset work, a capacitively coupled plasma torch array [2,9] is modeled by a lump circuit for numerical simulations. This model is first validated by showing good agreement between the numerical results of the discharge voltage and current and the corresponding experimental results for three cases of one to three torches being lit up in the array. It is then used to carry out simulations for a broad parameter space of plasma species. The results establish a dependence of power consumption on plasma parameters useful for minimizing the power budget for each application.

## **II. A Torch Plasma**

### ***A. Generation***

The plasma source investigated in the present work is an array of plasma torches produced by a capacitively coupled electrical discharge. Streams of compressed air blowing through an electrical discharge between pairs of electrodes form the plasma torches. The size of each torch for the present setup depends on the geometry of the electrode pair and the streaming speed of the air flow. Such an array of plasma torches can be made into the desired volume and plasma density and is particularly attractive because of the simplicity of its electronic circuitry, adaptability to any low frequency power source such as the 60 Hz from the wall outlet, and the flexibility of the panel design for the array. A schematic of a flat panel setup is shown in Fig. 1.

In general, all of the torches can be connected in parallel to a common power source if it has the required power handling capability. The capacitors in the circuit play a crucial role to the discharge. Without them, the torches in the set cannot be lit up simultaneously by a single common source. This is because once one is on, it tends to short out the voltage across all of the other electrode pairs connected in parallel. The capacitors work as active ballasting circuit elements. Charging and discharging of each capacitor provides feedback control to the voltage across the corresponding electrode pair.

### ***B. Voltage and Current Measurements***

From the voltage and current measurements, the average power consumption of the torch can be evaluated. It is found, and also confirmed by direct power measurement, to be about 350 Watts for a single torch. Moreover, one can also estimate the electron density of the torch plasma from the current measurement with the aid of the known geometry of the electrode pair [2,9]. Shown in Fig. 2a is an example of the measured gap voltage (solid curve) and loop current (dashed curve) as functions of time for a single torch case. The peak voltage and current, averaged over several runs, are found to be 2.8 kV and 2.5 A, respectively. Through such a voltage and current measurement, a dependence of gap voltage on loop current is determined and plotted in Fig. 3. It is shown that as the gap voltage exceeds the air breakdown voltage, the ionization rapidly increases

the conductivity of the gas so that the loop current increases while the gap voltage drops leading to a negative  $v-i$  characteristic. Hence, the discharge current is shown to be in the diffuse arc mode. A hysteresis phenomenon is also observed in the  $v-i$  curve. It is believed to be the result of heating, which changes the conductivity of the plasma and has a time delay from the variation of the discharge current (at 120 Hz). It is the gas flow that introduces a ballasting effect to prevent the constriction of the arc. Moreover, the  $v-i$  characteristics also explains why two torches can not be lit up simultaneously by a single power source, unless the ballasting capacitors are introduced in the circuit.

The gap voltage and loop current of each torch as functions of time are also measured for the cases of two coupled torches and three coupled torches. The results are presented in Fig. 2b and Fig. 2c, respectively. The results show that both voltage and current functions vary more rapidly with time as the number of coupled torches increases. Though their peak values seem to decrease, the duty factor of the current pulse in each half cycle, in fact, increases. It suggests that more plasma is produced by each torch when coupling is introduced. This may be explained by the increase of the power factor and by the reduction of the total harmonic distortion at the power line, indicating that the electrical performance of the circuit with coupled torches is significantly improved. Moreover, the coupling capacitors work as additional dependent sources providing feedback control of the discharge voltage and current of each torch so that the discharge can stay longer and the system operates with improved power efficiency.

### III. MODEL OF THE DISCHARGE

The role of the coupling capacitor is studied by modeling and simulating the electrical characteristics of the plasma torch. The simple geometry of the torch, two tungsten electrodes held end to end with a gas nozzle placed below to expel the discharge into free space, is considered. The discharge is then modeled by a lump circuit driven by a dependent voltage source. Each electrode pair is represented by a parallel RC circuit. Consider the simple geometry shown in Fig. 4 for the electrode pair, the equivalent resistance  $R_p$  and capacitance  $C_p$  of the electrode pair are derived to be [9]

$$R_p = \frac{v}{\omega_p^2 C_{p0}} \left( 1 + \frac{l}{d} \right) \left( 1 + \frac{l}{2a} \right) \quad (1)$$

and

$$C_p = C_{p0} + \frac{vd^2}{4\pi^2 R_p v_{te}^2} \left( 1 + \frac{l}{d} \right)$$

where both  $R_p$  and  $C_p$  are functions of the input voltage  $v$ , in addition to the dimensions and the geometry of the electrode pair (i.e., the radius  $a$  of the cylindrical electrodes and the separation  $d$  between two electrodes) and torch plasma (i.e., the height  $l$  of the torch);  $\omega_p$  is the electron plasma frequency,  $v_{te} = (T_e/m_e)^{1/2}$  the electron thermal speed, and  $C_{p0} = \epsilon_0 \pi a^2 / d$ . Thus, the equivalent lump circuit for a single torch is obtained as shown in Fig. 5 and serves as the building block for the equivalent circuit of the array of torches. Such an equivalent circuit is used to simulate and understand the operation of the torch array. It is done by solving the circuit equations with the aid of the experimentally measured  $v$ - $i$  characteristic shown in Fig. 3 for the dependent voltage function. The series inductor is included to model the hysteresis phenomenon observed in the  $v$ - $i$  curve. The hysteresis is believed to be the result of heating, which changes the conductivity of the plasma and has a time delay from the variation of the discharge current. The resistive component of the  $v$ - $i$  characteristic can be modeled mathematically by a function [9]

$$v = C_1 \tanh \alpha_1 i - C_2 \tanh \alpha_2 i \quad (2)$$

where constant parameters  $C_1$ ,  $\alpha_1$  and  $C_2$ ,  $\alpha_2$  are chosen to fit the functional curve of (2) to the experimental data of Fig. 3.

The lump circuit modeling the experimental setup (for three torches) to study the coupling between plasma torches in an array is shown in Fig. 6. This schematic shows all the electrical components used and their values, which will be utilized in the simulation. The simulation results of the gap voltage and loop current for the three cases of one, two, and three capacitively coupled torches are presented in Fig. 7. It is shown that the functional features of the experimentally measured results presented in Fig. 2 for the three cases are reproduced quite well by the numerical simulations.

In the single torch case, there is only one current pulse generated in each half period ( $T = 1/120$  sec.). It increases to two pulses for the three torch case. It is the result of coupling through the ballasting capacitors, which plays an important role in the operation of the torch array.

#### IV. POWER CONSUMPTION CALCULATION

The results of the simulations provide the necessary data for estimating the power consumption of the discharge. Plasma growth and decay are governed by the rate equations of plasma species [10] in each torch

$$\begin{aligned}\frac{dn_e}{dt} &= -v_a n_e + v_d n_- - \alpha n_e n_+ + v_i n_e \\ \frac{dn_+}{dt} &= -\alpha n_e n_+ - \beta n_+ n_- + v_i n_e \\ \frac{dn_-}{dt} &= v_a n_e - v_d n_- - \beta n_+ n_-\end{aligned}\quad (3)$$

where  $n_e$ ,  $n_+$ , and  $n_-$  are the densities of electrons, positive ions, and negative ions, respectively, in the unit of  $\text{cm}^{-3}$ ;  $v_a$  is the attachment rate and  $v_d$  is the detachment rate; and  $\alpha$  and  $\beta$  are the electron-ion recombination coefficient and ion-ion recombination coefficient, respectively, in the unit of  $\text{cm}^3 \text{sec}^{-1}$ . The gap voltage of the simulation is incorporated into Eq. 1 through the ionization frequency  $v_i$ , which represents the external driver of the discharge and is given by [11,12]

$$v_i = 383 v_a \left[ \epsilon^{3/2} + 3.92 \epsilon^{1/2} \right] e^{-7.546/\epsilon} \quad (4)$$

where  $\epsilon = E / E_{cr}$  is the discharge field normalized to the breakdown threshold field.

By solving Eq. 3, the net electron loss during a number of discharge periods can be evaluated. It turns out that the rate terms on the left hand side of Eq. 3 can be neglected in calculating the electron density decay. It is understandable because the temporal variation of the gap voltage is much slower than the transient variations of Eq. 3. The steady state solution of Eq. 3 is given by

$$\begin{aligned}n_e &= -\frac{v_d(\beta v_a + \alpha v_d - \beta v_i - \eta)}{\alpha(\beta v_a - (\alpha - 2\beta)v_d - \beta v_i + \eta)} \\ n_+ &= -\frac{\beta v_a - \alpha v_d - \beta v_i - \eta}{2\alpha\beta} \\ n_- &= \frac{v_d(\beta v_a + \alpha v_d - \beta v_i - \eta)}{\beta(\beta v_a - (\alpha - 2\beta)v_d - \beta v_i + \eta)}\end{aligned}\quad (5)$$

where  $\eta = \sqrt{4\alpha\beta v_d v_i + (\beta v_a + \alpha v_d - \beta v_i)^2}$  is used to simplify the presentation of (5).

The average power consumption is given by the average electron loss per second times the average ionization energy ( $\approx 10$  eV) of air [13]. Shown in Fig. 8 is a parametric dependence of the power consumption ( $\text{W}/\text{cm}^3$ ) on the average electron density ( $\text{cm}^{-3}$ ) maintained in the plasma, where the electron-ion recombination coefficient  $\alpha$  ( $\text{cm}^3\text{sec}^{-1}$ ) is used as a variable parameter. It provides a very useful reference for choosing the density regime for the most efficient operation of the plasma torch. The results for two situations are shown. The first is for a completely transient plasma generation system using Eq. 3, where an initial electron density is created and then allowed to recombine. The electron density is averaged over  $T = 1$  millisecond, which is shorter than the discharge duration of presently reported experiments, but yet very long to demonstrate a significantly different result from that of the second case. The second is for a steady state plasma generation system using Eq. 5. The large difference in the average power consumption between the two situations for each  $\alpha$  shows the importance of plasma maintenance, which can reduce the power budget considerably. The power consumption for the transient case can be reduced by increasing the repetition rate of the discharge (i.e., reducing  $T$ ). However, the engineering problem of the power supply becomes an issue. The simulation results also show that the power budget is reduced by decreasing the value of  $\alpha$ , which can be achieved by increasing the temperature of the plasma [14,15].

## V. SUMMARY

A lump circuit together with a dependent source representing the experimentally measured  $v$ - $i$  function is developed to model an array of plasma torches coupled to each other through ballasting capacitors. It is shown that the functional features of the experimentally measured results are reproduced quite well by the numerical simulations. Such an agreement provides the validation of the developed lump circuit model for simulating a complicated discharge system made up of coupled plasma torches.

Numerical simulations are then carried out for a broad parameter space of plasmas. The results of the simulations, coupled with the rate equations of the plasma species, provides the necessary data for estimating the power consumption of the discharge and for determining the parameter space for efficient generation and stable maintenance of the plasma. First, the numerical results show that the power consumption for plasma maintenance is much less than that for pulse generation. It suggests that a proper trigger mechanism for the start of plasma production may work to reduce the power requirement. Second, using the fitting curves of the simulation results, a function giving a parametric dependence of the consumed average power density  $\langle P \rangle$  on the normalized average electron density  $\langle n_e \rangle$  maintained in the plasma is derived to be  $\langle P \rangle = 48 \langle n_e \rangle^{1.9} \alpha^{0.4}$  (W/cm<sup>3</sup>), where  $\langle n_e \rangle$  is normalized to 10<sup>13</sup> cm<sup>-3</sup> and  $\alpha$ , the electron-ion recombination coefficient normalized to 10<sup>-7</sup> cm<sup>3</sup>sec<sup>-1</sup>, is the used as a variable parameter in the simulation. This relation provides a useful guide for the choice of the plasma density and temperature to achieve an efficient operation of the plasma torch.

#### **ACKNOWLEDGMENT**

This work is primarily funded by the Air Force Office of Scientific Research (AFOSR) grant AFOSR-F49620-97-1-0294 in cooperation with the DDR\&E Air Plasma Ramparts MURI Program.

## REFERENCES

- [1] R. J. Vidmar, "On the use of atmospheric pressure plasmas as electromagnetic reflectors and absorbers," *IEEE Trans. Plasma Sci.*, vol. 18, pp. 733-741, Aug. 1990.
- [2] E. Koretzky and S. P. Kuo, "Characterization of an atmospheric pressure plasma generated by a plasma torch array," *Phys. Plasmas*, vol. 5, no. 10, pp. 3774-3780, 1998.
- [3] M. I. Boulos, "Thermal plasma processing," *IEEE Trans. Plasma Sci.*, vol. 19, pp. 1078-1089, Dec. 1991.
- [4] J. R. Roth, *Industrial Plasma Engineering: Vol. I—Principles*, Institute of Physics Press, Bristol, 1995.
- [5] K. K. Wintenberg, T. C. Montie, C. Brickman, J. R. Roth, A. Carr, K. Sorge, L. Waslsworth, and P. Tsai, "Room temperature sterilization of surfaces and fabrics with one atmosphere uniform glow discharge plasma," *J. Industrial Microbiol. Biotechnol.*, vol. 20, pp. 69-74, 1998.
- [6] S. P. Kuo, I. M. Kalkhoran, D. Bivolaru, and L. Orlick, "Observation of shock wave elimination by a plasma in a Mach-2.5 flow," *Phys. Plasmas*, vol. 7, no. 5, pp. 1345-1348, 2000.
- [7] S. P. Kuo, E. Koretzky, and L. Orlick, "Design and electrical characteristics of a modular plasma torch," *IEEE Trans. Plasma Sci.*, vol. 27, pp. 752-758, June 1999.
- [8] S. P. Kuo, E. Koretzky, and R. J. Vidmar, "Temperature measurement of an atmospheric-pressure plasma torch," *Rev. Sci. Instruments*, vol. 70, no. 7, pp. 3032-3034, 1999.
- [9] E. Koretzky, "Atmospheric pressure plasma and electron cyclotron resonance plasma and their applications," Ph.D. dissertation, Polytechnic Univ., Brooklyn, NY 11201, Jan. 1999.
- [10] Y. S. Zhang and S. P. Kuo, "Bragg scattering measurement of atmospheric plasma decay," *Int'l J. IR & Millimeter Waves*, vol. 12, no. 4, pp. 335-343, 1991.
- [11] Y. A. Lupan, "Refined theory for an RF discharge in air," *Sov. Phys. Tech. Phys.*, vol. 21, no. 11, pp. 1367-1370, 1976.

- [12] S. P. Kuo and Y. S. Zhang, "Bragg scattering of electromagnetic waves by microwave produced plasma layers," *Phys. Fluids B*, vol. 2, no. 3, pp. 667-673, 1990.
- [13] S. C. Brown, *Basic Data of Plasma Physics*, M.I.T. Press, Cambridge, 1967.
- [14] L. G. Christophorou, *Electron-Molecule Interactions and Their Applications—Vol. 2*, Academic Press, Orlando, 1984.
- [15] B. R. Rowe, *Recent Flowing Afterglow Measurements, in Dissociative Recombination: Theory, Experiment and Applications*, Plenum Press, New York, 1993.

### Figure Captions:

Fig. 1 A schematic of a simple arrangement for an array of plasma torches. Tungsten electrodes are used. Each electrode pair is facilitated with an air jet nozzle.

Fig. 2 Experimental measurement of the plasma torch's voltage and current, for the three cases of (a) one torch, (b) two torches, and (c) three torches coupled with ballasting capacitors. The solid line is the voltage across the electrode gap and the dashed line is the current through the gap.

Fig. 3 Voltage-Current characteristic. The points are experimental values and the solid line is from the model.

Fig. 4 Dimensions of an electrode pair for the simply geometry.

Fig. 5 Lump circuit representation of the electrodes in the presence of the plasma torch.

Fig. 6 Schematic of the experimental setup used to study the coupling of plasma torches with ballasting capacitors.

Fig. 7 Simulation of the lump circuit representation of the plasma torch, for the three cases of (a) one torch, (b) two torches, and (c) three torches. The solid line is the voltage across the electrode gap and the dashed line is the current through the gap.

Fig. 8 Dependence of the average power consumption per cubic meter on the average electron density per cubic centimeter with the electron-ion recombination coefficient  $\alpha$  ( $\text{cm}^3\text{sec}^{-1}$ ) as a variable parameter. Solid lines are for transient plasma generation case and the dashed lines are for steady state plasma maintenance case.  $\alpha$  is given as (O)  $10^{-6}$ , ( )  $10^{-7}$ , and ( $\Delta$ )  $10^{-8}$ . ( $v_a = 4.56 \times 10^7 \text{ s}^{-1}$ ,  $v_d = 1.52 \times 10^7 \text{ s}^{-1}$ , and  $\beta = 1.2 \times 10^{-9} \text{ cm}^3 \text{ s}^{-1}$ )

Preceding Page Blank

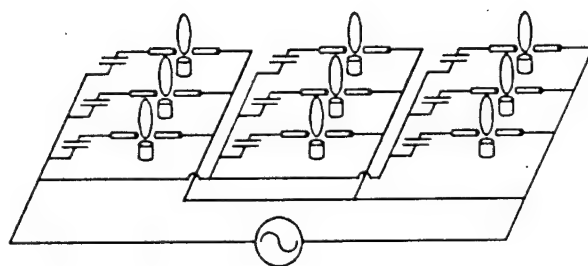


Fig. 1

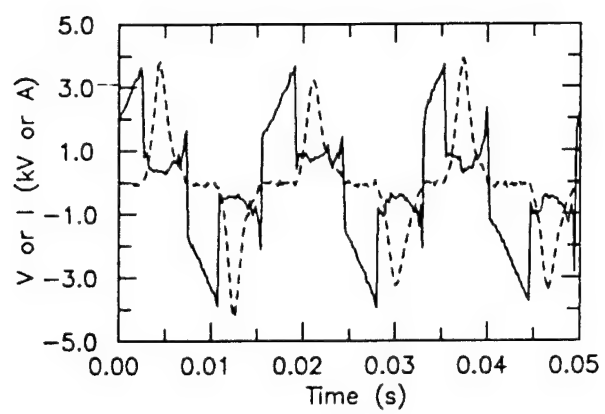


Fig. 2a

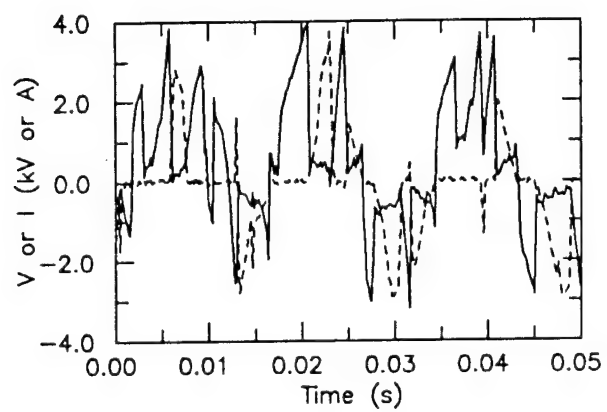


Fig. 2b

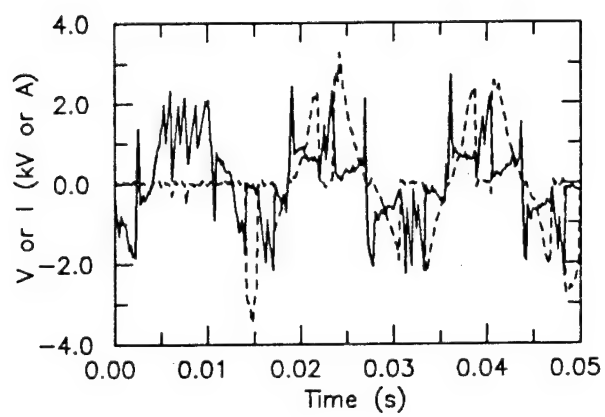


Fig. 2c

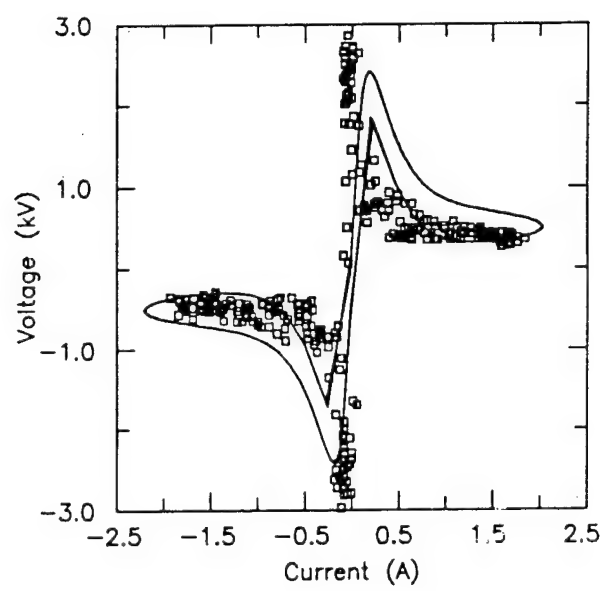


Fig. 3

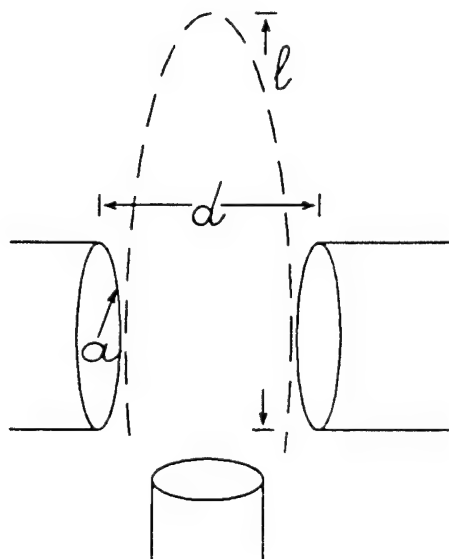


Fig. 4

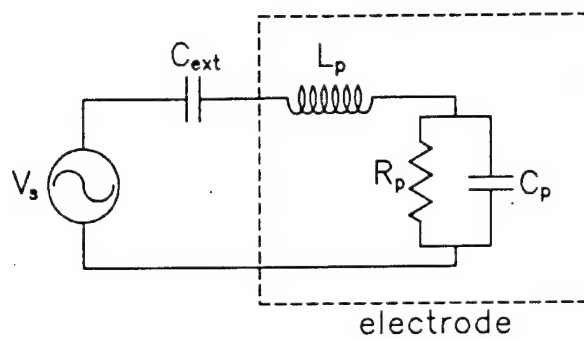


Fig. 5

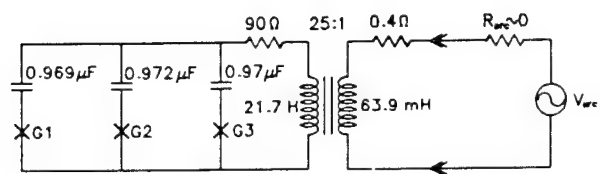


Fig. 6

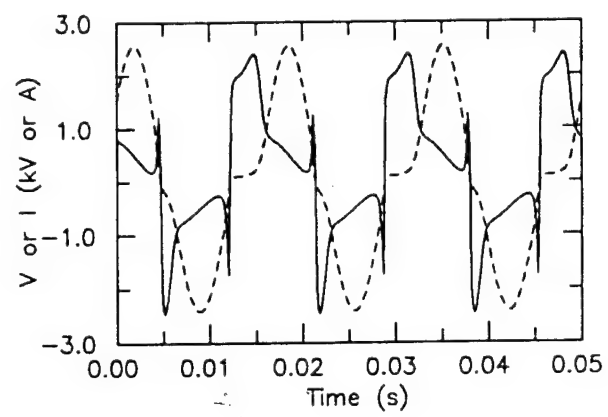


Fig. 7a

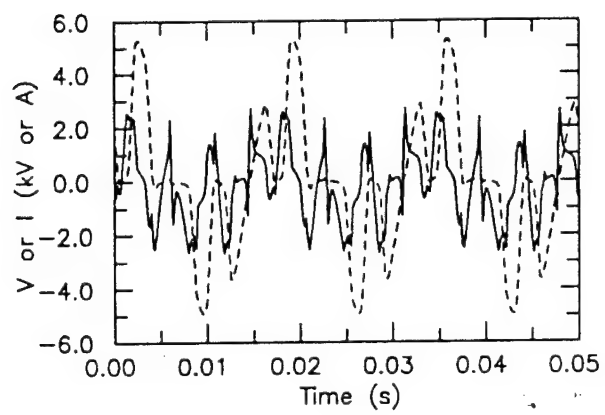


Fig. 7b

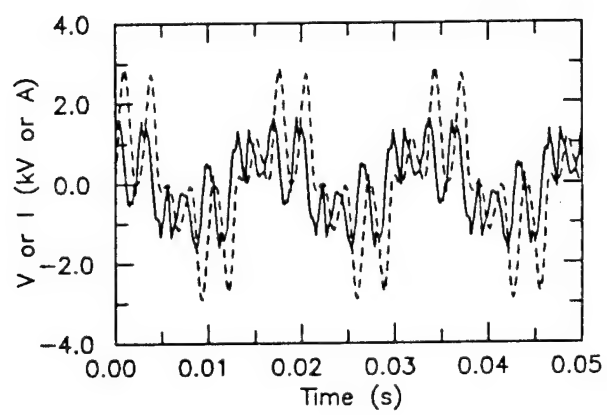


Fig. 7c

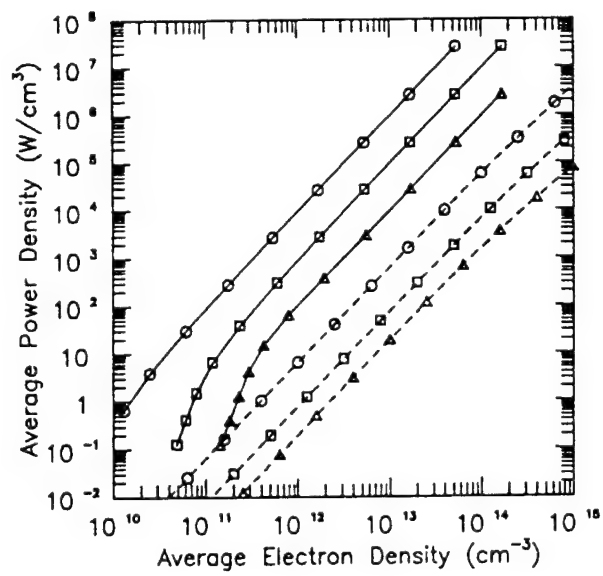


Fig. 8

# **The Effect of Plasma Aerodynamics on Shock Waves**

S. P. Kuo and Daniel Bivolaru

Department of Electrical Engineering, Polytechnic University

901 Route 110, Farmingdale, NY 11735

## **Abstract**

An experimental study of the plasma effect on the structure of an attached conical shock front appearing at the front end of a missile-shaped model has been carried out in a Mach-2.5 stream. The tip and the body of the model are designed as the cathode and anode, which are separated by a conical-shaped ceramic insulator providing a 5-mm gap for gaseous discharge. The electric field intensity near the cathode is enhanced by the sharpness of the tip. The experimental results show that the discharge can produce plasma distributed symmetrically around the tip in the region in front of the shock wave. It is observed that such plasma can cause the shock front to separate from the model. The shock wave moves upstream in the form of a detached bow shock becoming more and more diffusive and having an increasing shock angle as seen in the shadow video graphs of the flow. A physical mechanism of the observed plasma effect on shock wave is presented.

## I. Introduction

Shock waves have been the main obstacle for the development of supersonic/hypersonic vehicle. The very high wave drag associated with shock wave formation around a vehicle imposes restrictive vehicle shape requirements, which limit the flexibility of the vehicle design.

Moreover, shock waves formed around the supersonic/hypersonic vehicle have the side effect of producing sonic boom on the ground. The faster the vehicle is flying, the bigger the boom will be produced. The noise issue raises various environmental problems. They are serious enough to keep, for example, the Concorde supersonic jetliner from flying overland.

Therefore, if a technology for the attenuation or elimination of shock wave formation around a supersonic/hypersonic vehicle is developed, it will result in reduced fuel consumption and having smaller propulsion system requirements. The obvious commercial gain would be having larger payloads at smaller take-off gross weights and sonic boom attenuation during supersonic/hypersonic flight.

It is known that the propagation of a shock wave can be influenced by introducing an energy source to heat the gas temperature<sup>1,2</sup>. In these situations, heat is usually added to the approaching flow somewhere upstream of the model. Heat addition to the supersonic incoming flow results in a local reduction of Mach number which in turn causes the shock to move upstream and thus in this process the usually strong bow shock front is replaced by a weaker oblique shock with significantly lower wave drag. In addition, this shock wave merges with the original shock in the neighborhood of the model to form a significantly weaker oblique-type shock front<sup>3</sup>. Although this heating effect is an effective means of reducing the wave drag and sonic boom in supersonic and hypersonic flows, it requires a large power density to significantly elevate the gas temperature<sup>3</sup>. Thus, it is not an efficient approach for drag reduction purposes as it is known that using the thermal effect to achieve drag reduction in supersonic and hypersonic flight does not, in general, lead to energy gain in the overall process.

Therefore, plasmas have been suggested to possibly offer a non-thermal modification effect on the structure of the shock wave. It is based on the fact that an

important parameter affecting the shock wave is the speed of the sound, which depends on the temperature and the specific heats of the gas. Specific heats in turn relate to the complexity of the molecules comprising the gas. The electric forces among plasma particles may significantly modify the gas laws and thus, alter the aerodynamics of the vehicle flying through it. This suggestion was also based on the observation of early experiments conducted in shock tubes that the propagation velocity of shock waves in the glow discharge region is increased considerably<sup>4-7</sup>.

A pioneer experiment by Gordeev *et al.*<sup>8</sup> was carried out by injecting plasma into the flow through a nozzle of a cone-cylinder model placed in a supersonic stream. A significant drag reduction was reported. Then Ganguly *et al.*<sup>9</sup> carried out an experiment well equipped with laser diagnostics in the shock tube to distinguish the non-thermal effects from thermal effects<sup>3,10</sup>. The non-thermal effect of plasma on a supersonic stream was also observed in an experiment<sup>11</sup> investigating the relaxation time of the perturbation on the shock structure in decaying discharge plasma. The observed long-lasting effect on the shock structure was attributed to the exist of long-lived excited states of atoms and molecules in the gas.

To further demonstrate the plasma effect on the structure of shock waves, Kuo *et al.*<sup>12</sup> have carried out an experimental study in a Mach-2.5 wind tunnel. A missile-shaped model having a 60°-cone angle was placed in the test section of a Mach-2.5 wind tunnel. The tip and the body of the model were designed as the two electrodes, a modified structure from a plasma torch module<sup>13</sup>, which produced relatively low temperature<sup>14</sup> nonequilibrium plasma in open air, for gaseous discharge. A 60 Hz self-sustained diffused arc discharge generated spray-like plasma at the nose region of the model, where the usual attached conical shock was formed in the supersonic flow. The effect of the plasma on the shock wave formation was explored by examining a sequence of shadowgraphs taken during a typical wind tunnel run. The results showed that the introduced plasma could annihilate the shock wave at the nose region of the model. The peak and average power for plasma generation in this experiment were less than 1.2 kW and 100 W, respectively. Therefore, the thermal effect was not likely to be the cause mechanism.

In the present work, additional experimental evidences, obtained from experiments conducted prior to those presented in the Ref. 12, are presented to support the nonthermal plasma effect on the shock structure. A plausible physical mechanism explaining the experimental observations is also given.

## II. Experimental Setup and Plasma Characteristics

Experiments are conducted in the test section of a 15 in  $\times$  15 in supersonic blowdown wind tunnel shown in Fig. 1. The upstream flow has a flow speed  $v = 570$  m/s and a pressure  $p_1 = 1.8 \times 10^4$  Pa. A shock wave is produced in front of a missile-shaped model installed in the test section. Presented in Fig. 2 is a baseline shadowgraph of the flow field in the absence of plasma, showing a usual attached conical shock over the model. In this and other shadowgraphs presented in section III the flow is from left to right. The model is designed to have the tip and the body of the model as the two electrodes for gaseous discharge, which are separated by a conical-shape ceramic insulator providing a 5-mm gap. A 60 Hz power-supply in series with an rf trigger source is connected to the electrodes, in which the body electrode is electrically grounded through a connection with the bottom wall of the wind tunnel. The rf trigger is employed to generate the seed electrons for starting gaseous breakdown. Its output is a broadband rf signal having a peak voltage of 100 V. The breakdown voltage is provided by a power supply which includes a power transformer with a turns ratio of 1:25 to step up the line voltage of 120 V from a wall outlet to 3 kV, a 1  $\mu$ F capacitor in series with the electrodes, and a diode parallel to the electrodes to further step up the peak voltage. In the circuit, a 4 k $\Omega$  resistor is also connected in series with the diode preventing the charging current to exceed the specification of the diode. The circuit diagram is presented in Fig. 3.

During one of the two half cycles when the diode is forward biased, the capacitor is charged and the voltage across the electrodes is low. During the other half cycle, the diode is reversing biased. The charged capacitor increases the voltage across the electrodes and breakdown occurs. Thus the voltage across the electrodes has an asymmetric wave-form with a peak of about 4.5 kV, exceeding the 4 kV required for avalanche breakdown. Shown in Figs. 4a and b are a typical set of discharge voltage and current, and power functions of time, respectively, in the supersonic flow. The electric field intensity near the tip exceeds 10 kV/cm before breakdown occurs. It reduces to less than 1 kV/cm as the discharge current reaches the peak. It is shown in Fig. 4b that the peak power of the discharge is about 1.2 kW. The power of discharge is, however, negative in a period of time during each discharge cycle. This phenomenon was also observed in

running a torch plasma<sup>13</sup>, except the negative portion of the power function is much smaller in the torch case. It is possible due to the space charges accumulated in the plasma that become a source. The average power (<100 W) in the present case is also much less than that ( $\approx 230$  W) consumed in the torch plasma. Since discharge only occurs during one of the two half cycles, one can designate the tip electrode as a cathode or an anode by simply adjusting the orientation of the diode in the connection. It was found that significant modification of shock structure appeared only when the tip of the model was designated as the cathode<sup>12</sup> and the discharge was symmetric around the tip of the model. As shown by the video graph in Fig. 5a, such an arrangement produced spray-like plasma around the tip. This was because the discharge could pass through the shock front into the lower pressure region. It is noted that a filter has been used to cut down the airglow intensity. Consequently, the plasma image shown in Fig. 5a as well as others presented in the following appears to be much smaller than those unfiltered plasma images presented in the previous work<sup>12</sup>. The corresponding shadowgraph of the flow field is presented in Fig. 5b. Comparing this shadowgraph in Fig. 5b with the baseline shadowgraph in Fig. 2, significant plasma effect on shock wave is clearly observed. However, the discharge could be asymmetric. In this situation, the plasma as shown in Fig. 5c was usually produced in the region behind the shock front near the surface of the model. Thus, the generated plasma had very little effect on the shock wave. This is demonstrated by the corresponding shadowgraph of the flow field presented in Fig. 5d. It is noted that the discharge in this case was strong as indicated by the intense background light of the shadowgraph. In the other arrangement with the tip as the anode, the discharge was usually asymmetric around the tip and the generated plasma was distributed near the surface of the model.

Two video cameras are used to monitor experiments. One records the spatial distribution and temporal evolution of the plasma through its airglow image. The other one tapes the shadow video graph of the flow. The results extracted from the videotapes of the shadow image of the flow and the airglow images of the plasma provide crucial information on the correlation between plasma distribution and modification of shock structure. Moreover, continuous shadowgraphy of the flow reveals important information regarding the transient behavior of the flow field.

### III. Observations

The experiments presented in the following were conducted prior to those presented in the Ref. 12 and the Pitot probe was not yet installed. As a plasma is introduced through a discharge at the tip region of the shock-generating cone with the tip of the model designated as the cathode, the shadowgraph of the flow field is found to be different from that shown in Fig. 2. The effect of the plasma on the structure of the shock front also depends on the density and volume of the plasma produced by the discharge, which varies with time. Since the discharge is 60 Hz and the video camera records at a rate of 30 frames per second, the temporal variation of the shock wave structure during a single discharge period can not be recorded directly. A time assembly approach is adopted to reconstruct time dependence of shock structure.

A time sequence of four shadowgraphs taken during the off and on period of plasma in the middle of a wind tunnel run is presented in Figs. 6a to 6d. These shadowgraphs form a time assembly set resembling the temporal evolution of the shock wave structure during a discharge period. The corresponding plasmas produced by discharges are shown in Figs. 6e to 6h. First shadowgraph shown in Fig. 6a is for the case that the discharge is off as indicated by Fig. 6e. Therefore, the shadowgraph is dark (lack of background light from plasma) and similar to the baseline one presented in Fig. 2. The next one presented in Fig. 6b corresponds to the case that the discharge is near or reaches the peak. The produced plasma shown in Fig. 6f is distributed symmetrically near the tip. The strong plasma effect on shock wave presented in Fig. 5b is again observed in Fig. 6b, showing that shock wave becomes very diffusive and has a much larger shock angle. The following two shadowgraphs in Figs. 6c and 6d are showing the recovery of shock wave from the plasma perturbation as the discharge decays from its peak to those shown in Figs. 6g and 6h. Although the discharge shown in Fig. 6g seems weaker than that shown in Fig. 6h, it is focused in the center around the tip of the model and introduces stronger perturbation to the shock wave structure than that introduced by the one shown in Fig. 6h. The shadowgraph of Fig. 6d is similar to that presented in Fig. 5d, showing negligible plasma effect on shock wave. The corresponding plasma shown in Fig. 6h is also similar to that shown in Fig. 5c, having an asymmetric distribution around the tip of the model. On

the other hand, a comparison of Figs. 6c and 6a clearly observes a larger shock angle indicating a transformation of the shock from a well defined attached shock into a classic highly-curved bow shock structure. The diffused form of the shock front could be an indication of shock wave being weakened by the plasma. However, it is noted that due to the non-uniformity of the generated plasma the shock front could be perturbed to an asymmetric form. Thus, the integration effect inherent in the shadowgraph technique when visualizing a three-dimensional flow field could also lead to the observed diffused form of the shock front. This phenomenon is commonly observed when the spatial extent of the region leading to the shock is small compared to the test section dimensions, which is, however, not the case of the present experiment.

The pronounced influence of plasma on the shock structure is clearly demonstrated by the result showing in Fig. 6b. This one together with the one presented in Fig. 5b are encouraging results, which may have significant consequences in the effectiveness of this plasma scheme in minimizing wave drag at supersonic speeds. These observations were typical of all the experiments performed. Due to cyclic nature of the generated plasma, however, an unsteady shock motion containing the above-mentioned features of the flow field (Figs. 6a to 6d) is seen in the recorded videotape.

#### IV. Discussion

The tip and the body of a missile-shaped model are designed as the two electrodes for gaseous discharge. The sharpness of the tip helps to enhance the electric field intensity in the region in front of the tip. Moreover, the tip of the model is arranged as the cathode. This arrangement together with the favorable electric field distribution make electron current in the discharge much easier to pass through the shock front into the upstream (lower pressure) region before returning to the body of the model as the anode. The plasma, produced by local discharge in the upstream region, as seen by its airglow image is distributed symmetrically around the tip.

Since the applied electric field extends to the region upstream of the baseline shock front, the local field can continuously accelerate the plasma electrons in the upstream region in the direction opposite to the flow direction. Some of them will gain enough energy for ionization and others deflect the propagation direction of molecules in the incoming flow via momentum transfer collisions. The average momentum transfer from electrons to each molecule in the flow is given by  $\Delta P = v_{en} t_n (n_e/n_N) P_e$ , where  $v_{en} \sim 1.9 \times 10^{12} \sqrt{\epsilon_e} \text{ s}^{-1}$  is the electron-neutral particle collision frequency,  $\epsilon_e$  is the electron energy in the unit of eV,  $t_n = l/v = 3.5 \times 10^{-5} \text{ s}$  is the transit time of the flow passing through a 2 cm plasma layer,  $n_e$  and  $n_N$  are the electron and flow density, and  $P_e$  is the magnitude of the electron momentum. Similarly, the average energy transfer through the elastic collision process is given by  $\Delta \epsilon \sim v_{en} t_n (n_e/n_N) (2m_e/m_N) \epsilon_e$ , where  $m_e$  and  $m_N$  are the masses of the electron and neutral particle, respectively. It is noted that the inelastic collision is a very effective channel for energy deposition in air. However, most of the stored energy in the excited-molecules is carried away by the speedy flow before being thermalized for heating. Thus, the contribution of inelastic collisions is not included in an estimate of energy transfer for heating. A more detail reasoning is given in the next paragraph. The relative importance of the deflection effect via momentum transfer collisions and the heating effect of the plasma on the incoming flow can be determined by the ratio  $(\Delta P/P_n)/(\Delta \epsilon/\epsilon_N)$  of the normalized momentum transfer to the normalized energy transfer, where  $P_n = m_N v$  and  $\epsilon_N = 3k_B T_N/2 = 1.68 \times 10^{-2} \text{ eV}$  are the momentum and thermal energy of a molecule ( $N_2$ ) in the flow. It is noted that the dominant momentum transfer effect is to deflect the

propagation direction of molecules in the flow, which is not necessary to reduce the momentum of molecules in the flow direction. A cartoon figure to illustrate the process is presented in Fig. 7. This process is most effective when plasma has a symmetric distribution around the tip. The additional experimental evidences showing in Fig. 8 support it. The two sets of shadowgraph/plasma image shown in Fig. 8 together with the other two sets presented in Figs. 5b/5a, and 6b/6f, are all showing that a symmetrically distributed plasma gives rise to the strongest plasma effect on shock wave. Since  $(\Delta P/P_n)/(\Delta \epsilon/\epsilon_n) \sim (1/2)(m_n \epsilon_N/m_e \epsilon_e)^{1/2} \cong 15/\sqrt{\epsilon_e} \geq 5$  (for  $\epsilon_e < 10$  eV limited by the ionization process), the deflection effect dominates over the heating effect. This explains why the peak and average power consumed in the electric discharge have unexpected low values (1.2 kW and 100 W, respectively). Moreover,  $\Delta P/P_n \sim 1.2 \underline{n_e} \epsilon_e$  has a value of the order of 1, where  $\underline{n_e} \sim 1$  is the electron density<sup>15</sup> in the unit of  $10^{13} \text{ cm}^{-3}$ . As a result, the shock front moves upstream toward the plasma front and becomes more and more dispersed in the process.

As mentioned before, inelastic collisions are very important for energy deposition in air. However, those excited molecules move with high speeds and the region of interest (i.e., around and behind the tip of the model) is very small. The transit time of gas passing through that region is less than 20  $\mu\text{s}$ . During this time period, unthermalized excited-molecules will just carry the stored energy away. In other words, inelastic collision is a good channel to remove the input energy of the discharge from the region of interest, rather than for heating the gas in the region of interest. Thus its contribution is not included in the analysis presented in the preceding paragraph.

To further justify the conclusions based on the results of the preceding analysis, the first principle "conservation of energy" is used for an estimate of the gas temperature enhancement caused by the discharge. An ideal case assuming 100% energy transfer for heating is considered for over estimation.

Assuming that the gas temperature in the region of discharge is increased by  $\Delta T$ . This region has a cross section area  $A$  to the open region. Therefore, the power loss in this heated region is given by  $P_L = A n v \Delta T$ , owing to heated gas moving out of the region and replaced by unheated gas, where  $n$  and  $v$  are the density and flow speed of the gas. In

steady state, this thermal power loss has to be compensated by the power input (assuming 100% thermalization), leads to

$$An v \Delta T = P_{in}$$

In the region behind the shock front,  $v \cong 300$  m/s,  $n \cong 4.5 \times 10^{25} \text{ m}^{-3}$ ,  $A \cong 2\pi \times 5\text{mm} \times 8\text{mm} = 2.4 \times 10^{-4} \text{ m}^2$ , thus the peak and average temperature enhancements are obtained as  $\Delta T_{\text{peak}} \cong 26$  K (for  $P_{in|_{\text{peak}}} = 1.2$  kW) and  $\Delta T_{\text{ave}} \cong 2.2$  K (for  $P_{in|_{\text{average}}} = 100$  W).

Therefore, the peak temperature perturbation in the ideal case is less than 10% of the unperturbed temperature 285 K in the region behind the shock and less than 20 % of the ambient free stream gas temperature 135 K and the average temperature perturbation is less than 1% and 2 %, respectively. If the power carried away by non-thermalized excited-molecules is also taken into account, the estimated temperature perturbation will be even smaller.

The effect of plasma aerodynamics on the shock wave observed in the experiments may be understood physically. Shock is a nonlinear wave of a supersonic flow. In the steady state, when the input provided by the incoming flow is balanced out by the wave dissipation in the flow, a sharp shock front noticed by a step pressure jump is formed to separate the flow into regions of distinct entropies. Conceptually, an easy way to move the shock wave upstream is to set up a new shock in front of the location of the original one. Introducing a plasma spike deflecting the propagation direction of the incoming flow before the flow reaches the tip of the model can do it. Thus the pressure of the flow in the region slightly upstream of the original shock front can build up to form a new shock front. As the process continues, the shock front is expected to move upstream. The shock front is also expected to appear in a dispersed form because the effective plasma spike is distributed spatially and is not as rigid as the tip of the model. The strength of the shock wave is weakening in the process because the plasma spike introduces additional lateral spread of the incoming flow.

**Acknowledgments**

We would like to acknowledge Dr. Skip Williams, Air Force Research Laboratory (AFRL) at Hanscom, MA and Professor Iraj M. Kalkhoran, Polytechnic University, for the useful discussions and for their interest and valuable comments on the manuscript. We would also like to thank Mr. Lester Orlick for his help in running the wind tunnel and machining the model.

This work was primarily supported by the Air Force Office of Scientific Research (AFOSR) Grant AFOSR-F49620-97-1-0294 in cooperation with the DDR&E Air Plasma Ramparts MURI Program.

## References:

1. D. M. Bushnell, AIAA Paper 90-1596, June (1990), American Institute of Aeronautics and Astronautics, Washington DC.
2. D. S. Miller and H. W. Carlson, AIAA Paper 70-903, July (1970), American Institute of Aeronautics and Astronautics, Washington DC.
3. D. Riggins, H. F. Nelson, and E. Johnson, AIAA J. **37**, 460 (1999).
4. A. N. Klimov, A. N. Koblov, G. I. Mishin, Yu. L. Serov, and I. P. Yavov, Sov. Tech. Phys. Lett. **8**, 192 (1982).
5. A. N. Klimov, A. N. Koblov, G. I. Mishin, Yu. L. Serov, K. V. Khodataev, and I. P. Yavov, Sov. Tech. Phys. Lett. **8**, 240 (1982).
6. I. V. Basargin and G. I. Mishin, Sov. Tech. Phys. Lett. **11**, 85 (1985).
7. P. A. Voinovich, A. P. Ershov, S. E. Ponomareva, and V. M. Shibkov, High Temp. **29**, 468 (1990).
8. V. P. Gordeev, A. V. Krasilnikov, V. I. Lagutin, and V. N. Otmennikov, Fluid Dynamics **31**, 313 (1996).
9. B. N. Ganguly, P. Bletzinger, and A. Garscadden, Phys. Lett. A **230**, 218 (1997).
10. F. Marconi, AIAA Paper 98-0333, Jan. (1998), American Institute of Aeronautics and Astronautics, Washington DC.
11. A. S. Baryshnikov, I. V. Basargin, E. V. Dubinina, and D. A. Fedotov, Tech Phys. Lett. **23**, 259 (1997).
12. S. P. Kuo, Iraj M. Kalkhoran, Daniel Bivolaru, and Lester Orlick, Phys. Plasmas **7**, 1345 (2000).
13. S. P. Kuo, E. Koretzky, and L. Orlick, IEEE Trans. Plasma Sci. **27**, 752 (1999).
14. S. P. Kuo, E. Koretzky, and R. J. Vidmar, Rev. Sci. Instruments **70**, 3032 (1999).
15. E. Koretzky and S. P. Kuo, Phys. Plasmas **5**, 3774 (1998).

### Figure Captions:

Figure 1. A Mach-2.5 wind tunnel.

Figure 2. A baseline shadowgraph of the flowfield in the absence of plasma.

Figure 3. A schematic of the circuit for the electric discharge.

Figure 4. (a) Normalized discharge voltage  $V(t)$  and current  $I(t)$ . The actual voltage and current are given by  $150 \times V(t)$  volts and  $0.41 \times I(t)$  amperes. (b) Power function  $P(t)$  of the discharge.

Figure 5. (a) Plasma produced in front of the model with a symmetric distribution around the tip of the model, (b) the corresponding shadowgraph of the flow field showing strong plasma effect on shock wave, (c) plasma has an asymmetric distribution around the tip of the model, and (d) the corresponding shadowgraph of the flow field showing negligible plasma effect on shock wave.

Figure 6. A time sequence of four shadowgraphs (a)-(d) taken during the off and on period of plasma in the middle of a wind tunnel run at Mach 2.5. The plasmas corresponding to the shadowgraphs in (a)-(d) are shown in (e)-(h), respectively.

Figure 7. Cartoon showing the envisioned field distribution supporting the discharge and the deflection of the incoming flow by the discharge-produced plasma.

Figure 8. Two sets of shadowgraph/plasma image showing consistently that only symmetric distributed plasmas give rise to significant plasma effect on shock wave.



Fig. 1

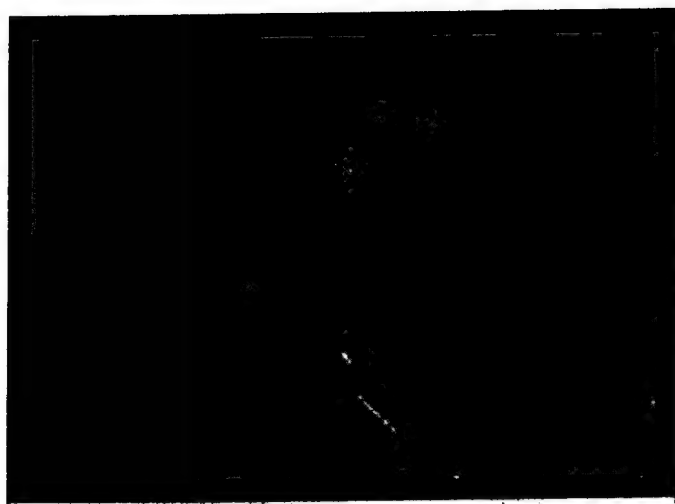


Fig. 2

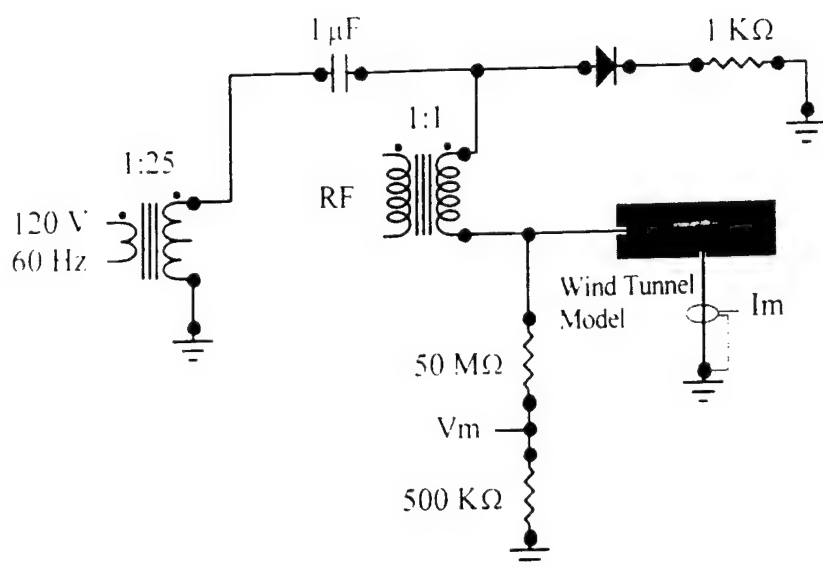
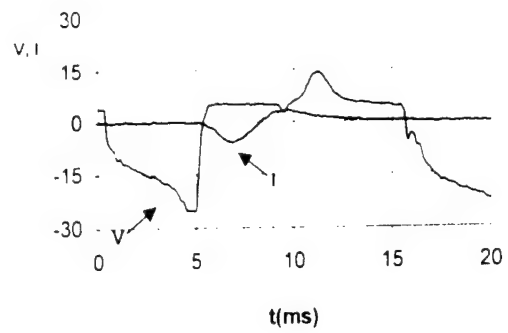
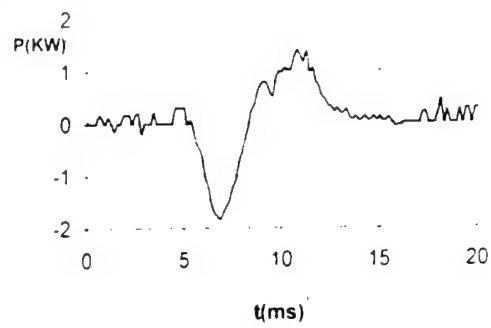


Fig. 3

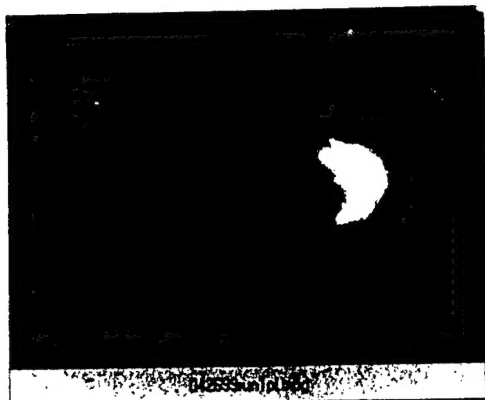


(a)

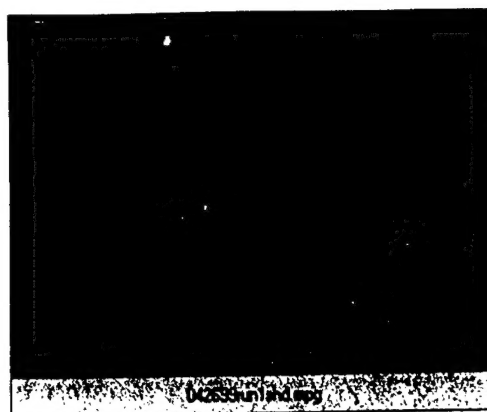


(b)

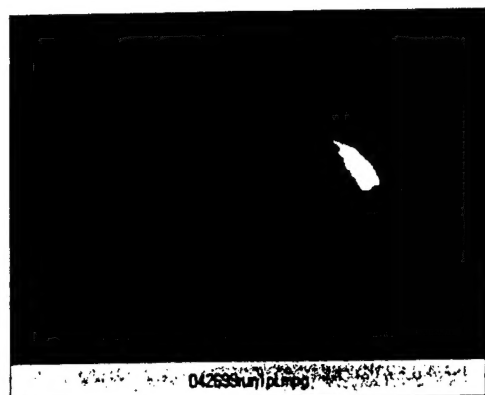
Fig. 4



(a)



(b)

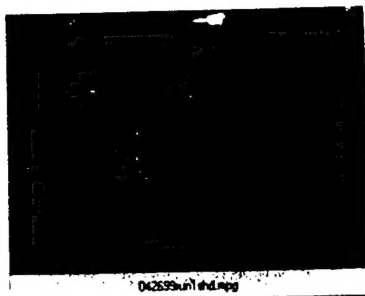


(c)

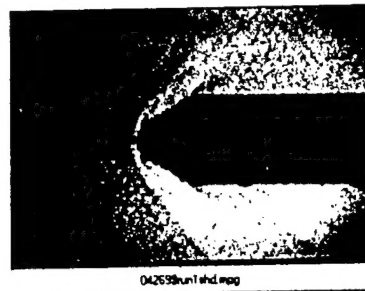


(d)

Fig. 5



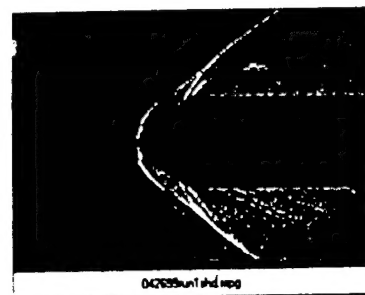
(a)



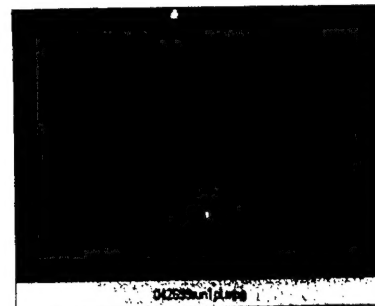
(b)



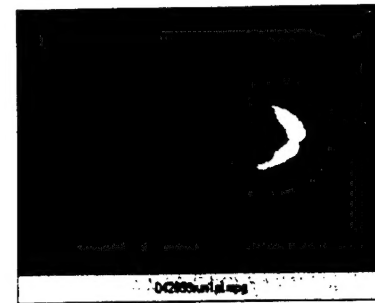
(c)



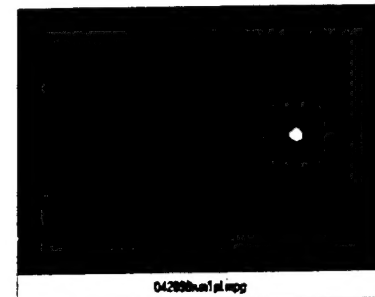
(d)



(e)



(f)



(g)



(h)

Fig. 6

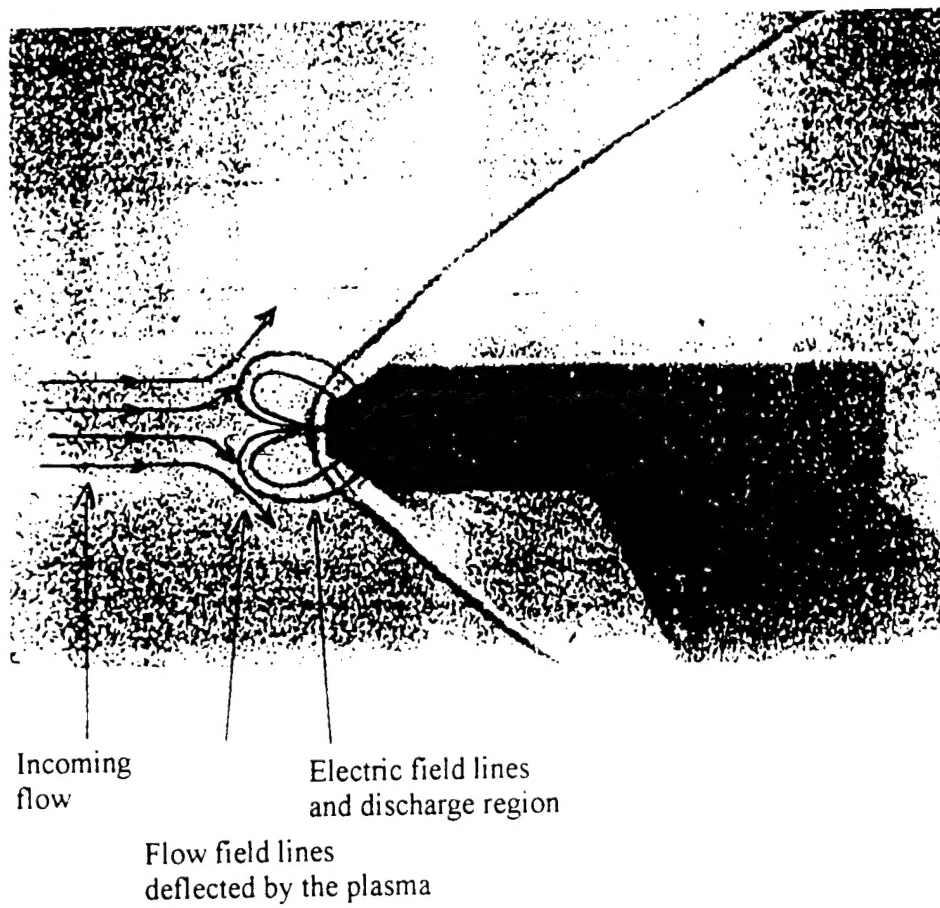


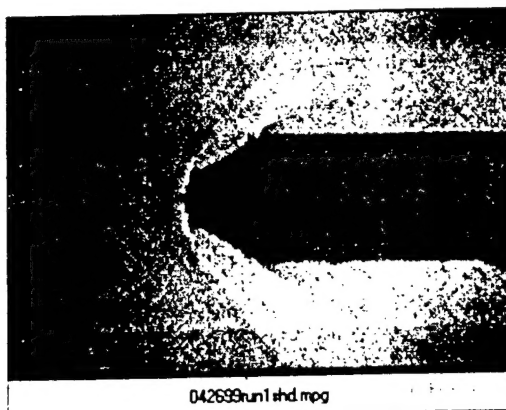
Fig. 7



(a)



(c)



(b)



(d)

Fig. 8